

Electronic Supplementary Information

Reversible Uncompetitive Inhibition of Metal-Organic Framework Nanozymes: Specific Colorimetric Assay of Methidathion without Enzymes

Haiying Chen, Xin Zhang, Weimin Gao, Baojian Huang, Lei Han*

College of Chemistry and Pharmaceutical Sciences, Qingdao Agricultural University,
Qingdao 266109, Shandong, China.

* Corresponding Author.

E-mail address: hanlei@qau.edu.cn

Contents

Experimental Section	S3
Fig. S1. Synthesis schematic of Fe-MOF	S7
Fig. S2. N ₂ adsorption-desorption isotherm.....	S7
Fig. S3. Absorbance curves at 652 nm with time for Fe-MOF-catalyzed TMB oxidation.....	S8
Fig. S4. The pH-dependent oxidase-like activity of Fe-MOF	S8
Fig. S5. Time-dependent absorbance change of reaction solution catalyzed by Fe-MOF in the presence of methidathion	S9
Fig. S6. (A) Double reciprocal plot and (B) Michaelis-Menten curve for enzyme kinetics of Fe-MOF.....	S10
Fig. S7. (A) Double reciprocal plot and (B) Michaelis-Menten curve for enzyme inhibition kinetics of Fe-MOF with 0.5 μM of methidathion	S11
Fig. S8. (A) Double reciprocal plot and (B) Michaelis-Menten curve for enzyme inhibition kinetics of Fe-MOF with 1 μM of methidathion.....	S12
Fig. S9. Schematic of the steady-state equilibrium for uncompetitive inhibition.....	S13
Fig. S10. Absorbance spectra of various reaction systems for oxidase-like activity of Fe-MOF.	S13
Fig. S11. The activities of Fe-MOF after incubation with the various pesticides.....	S14
Fig. S12. Photograph of the reaction system with various concentrations of methidathion	S15
Fig. S13. Signal response of the colorimetry system for methidathion detection in the presence of (A) other pesticides (0.1 mM) and (B) metal ions (0.1 mg/mL).....	S15
Table S1. Performance comparison of various analytical methods.....	S16
Table S2. Determination of methidathion in real samples.....	S17
References	S18

Experimental Section

Reagents and materials. $\text{FeCl}_2 \cdot 4\text{H}_2\text{O}$ was bought from Sinopharm Chemical Reagent. Benzenedicarboxylic acid (BDC), Triethylamine (TEA) and N, N-dimethylformamide (DMF) were purchased from Aladdin Reagent. 3,3',5,5'-tetramethylbenzidine (TMB) was bought from Shanghai Macklin Biochemical Technology Co., Ltd. Methidathion and hydroethidine (HE) were bought from Sigma Aldrich. All other reagents were of analytical grade and used without further purification. All aqueous solutions were prepared with ultrapure water (18.2 M Ω cm) from a Milli-Q system (Millipore, Germany).

Apparatus. Transmission electron microscopy (TEM) was performed with a TEM H-7650 (Hitachi, Japan), and sample was prepared by dropping the diluted solutions onto copper grids and then drying at room temperature. The crystal structure of the material was identified by X-ray diffraction (XRD) D8ADVANCE (Bruker, Germany). The elementary composition and valence state of the materials were analyzed via an X-ray photoelectron spectroscopy (XPS) ESCALAB 250Xi instrument (Thermo Fisher Scientific, USA). The Brunauer-Emmett-Teller (BET) surface area and pore size were measured using ASAP 2020 Plus (Micromeritics, USA). The spectrophotometric assay was accomplished using ultra-sensitive multi-function microchannel plate detector CYTATION (Biotek, USA). Fluorescent spectra were recorded using a fluorescence spectrophotometer F-7000 (Hitachi, Japan). The thermogravimetric analysis (TGA) was done on Simultaneous thermal analyzer SDT650 (WATERS, USA) with a heating rate of 10 °C min⁻¹ from 50 to 800 °C under nitrogen atmosphere. Electron spin

resonance (ESR) was performed with BRUKER EMXPLUS (Karlsruhe, Germany).

Synthesis of Fe-MOF. Firstly, DMF (32 mL), ethanol (2 mL) and ultrapure water (2 mL) were mixed in a centrifuge tube (50 mL). Secondly, BDC (0.75 mmol) was dissolved into the above mixture under ultrasonication. Next, $\text{FeCl}_2 \cdot 4\text{H}_2\text{O}$ (0.375 mmol) was added and dissolved in the above mixture. Then, TEA (0.8 mL) was immediately injected into the above solution. Afterwards, the mixture was stirred for 5 min to achieve a colloidal solution. After the continuous ultrasonication for 8 h (40 kHz) under sealed condition, the well-distributed colloidal suspension was obtained. Lastly, the products were centrifugated, washed with water and ethanol, and dried at room temperature for subsequent use.

Oxidase-like activity assay of Fe-MOF. Typically, Fe-MOF (0.1 mg/mL) were added to acetate buffer (0.1 M, pH 4.0) containing chromogenic substrate TMB (0.5 mmol L⁻¹). The reaction was carried out under the different concentrations of O₂ atmospheres for 30 min at room temperature, and the absorbances of the corresponding oxidization products (oxTMB at 652 nm, oxOPD at 450 nm) were detected after ending the reaction by centrifugation. Each experiment was repeated three times.

The effect of pH on the oxidation-mimicking activity of Fe-MOF nanozymes was also investigated by the above method, apart from varying the pH (pH 3.0–9.0). The temperature stability of Fe-MOF was evaluated by the above assay after Fe-MOF was incubated at different temperatures (4, 25, 37, 50, 60, 70, and 80 °C) for two hours.

Detection of the superoxide radicals. To research the possible generation of the superoxide radicals ($\bullet\text{O}_2^-$) in the catalytic reaction, different concentrations of Fe-MOF

were added into acetate buffer (0.1 M, pH 4.0), and then HE (0.5 mM, final concentration) was added into the above solution. After incubation for 30 min, the fluorescence spectra were recorded ($\lambda_{\text{ex}} = 470 \text{ nm}$, $\lambda_{\text{em}} = 590 \text{ nm}$).

Enzyme kinetics assay of catalyst and inhibition. The steady-state kinetics analysis for the oxidase-like activity of Fe-MOF (0.1 mg/mL) was conducted by changing the concentrations (0.05, 0.06, 0.1, 0.3, 0.5, 0.6, 1, and 1.2 mmol L⁻¹) of TMB. The absorbance at 652 nm was determined over a period of time to obtain the initial reaction rates. For obtaining the apparent kinetic parameters (K_m and V_{max}), the data were fitting by the Michaelis-Menten equation.

The inhibition kinetics for the oxidase-like activity of Fe-MOF by methidathion were investigated by the above steady-state kinetics analysis method in presence of the different concentrations of methidathion (0.5 and 1 μM).

Statistical analysis. For statistical analysis, all of the experiments were repeated at least three times. For each test, mean \pm standard deviation was calculated. Statistical analyses were accomplished using GraphPad Prism Version 9.5.1 (GraphPad Software, USA). Statistical significance was concluded by a one-way analysis of variance (ANOVA), and P values less than 0.05 were thought to be statistically significant.

Colorimetric assay of methidathion. Firstly, different concentrations of methidathion (0.01, 0.05, 0.1, 0.2, 0.3, 0.4, 0.5, 0.6, 0.8, 0.9, 1, 1.2, and 1.4 μM) were incubated with Fe-MOF (0.1 mg/mL) for 10 min, respectively. Afterwards, acetate buffer (0.1 M, pH 4.0) containing TMB (0.5 mM) was added to the above solutions. After incubation at room temperature for 15 min, the color change of the above mixture

could be photographed, and the absorbance was determined at 652 nm. Each experiment was performed in triplicate. The calibration curve was plotted by the linear fitting.

Methidathion detection in real samples. For the applicability evaluation of the proposed colorimetric assay method, environmental waters (tap water, river water, and sea water) were used as the real samples. The recovery was acquired by a standard addition assay. The real samples were pretreated by filtering with 0.22 μm membranes. After diluting with acetate buffer (0.1 M, pH 4.0) to fit into the linear range of the calibration curve, the sample solutions were explored by the proposed assay method. Each sample was independently measured five times.

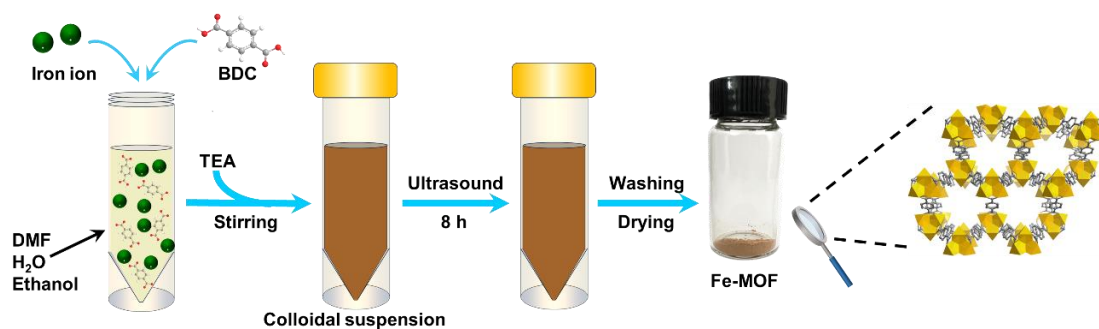


Fig. S1. Synthesis schematic of Fe-MOF.

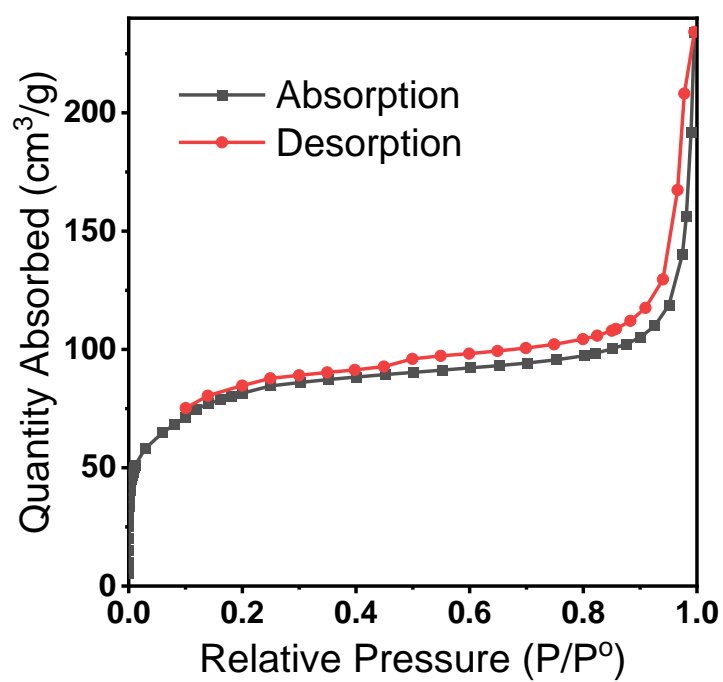


Fig. S2. N₂ adsorption-desorption isotherm.

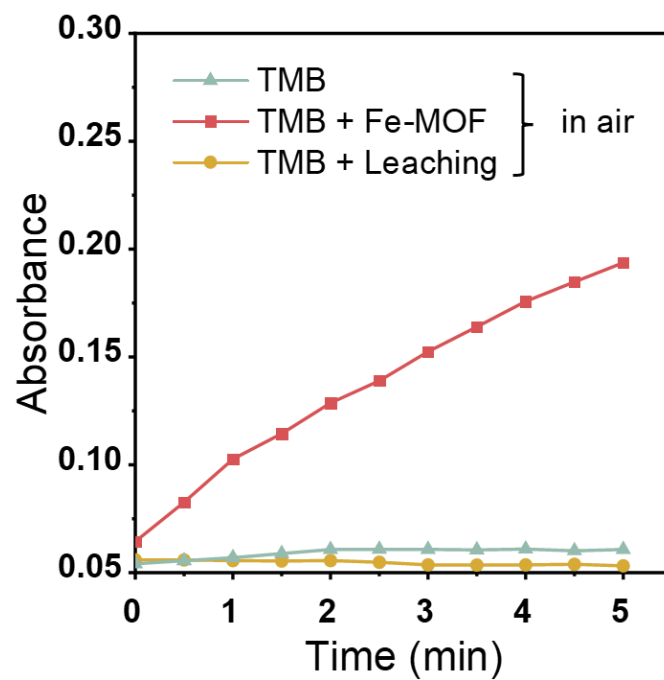


Fig. S3. Absorbance curves at 652 nm with time for Fe-MOF-catalyzed TMB oxidation.

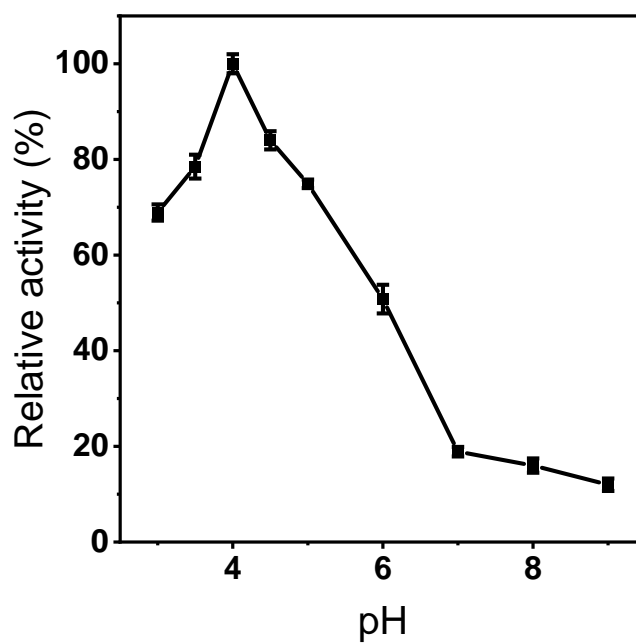


Fig. S4. The pH-dependent oxidase-like activity of Fe-MOF.

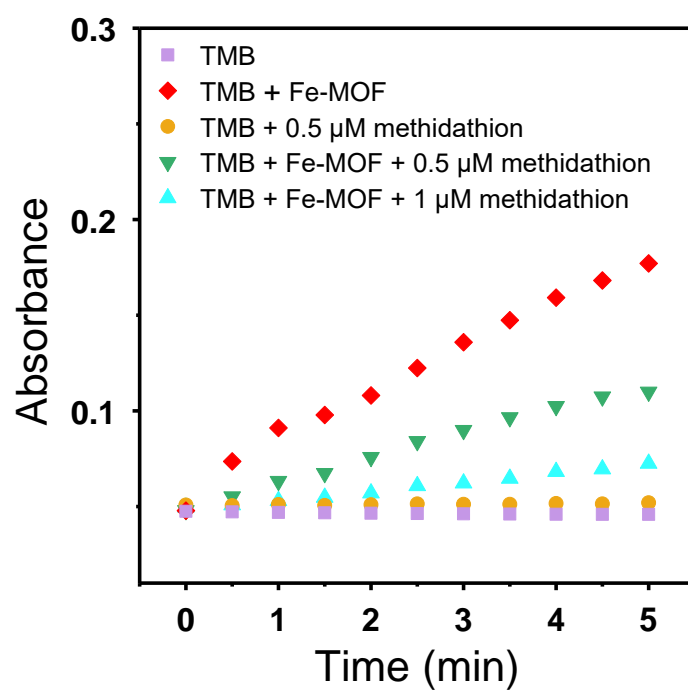


Fig. S5. Time-dependent absorbance change of reaction solution catalyzed by Fe-MOF in the presence of methidathion.

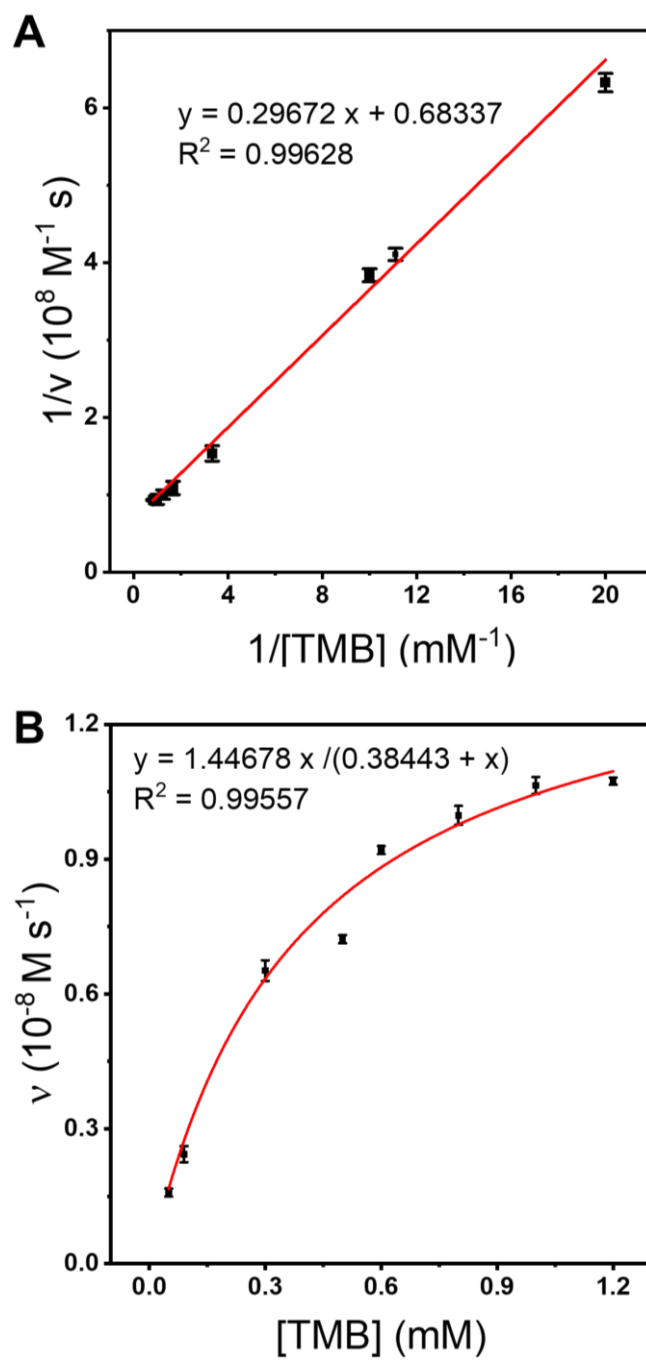


Fig. S6. (A) Double reciprocal plot and (B) Michaelis-Menten curve for enzyme kinetics of Fe-MOF.

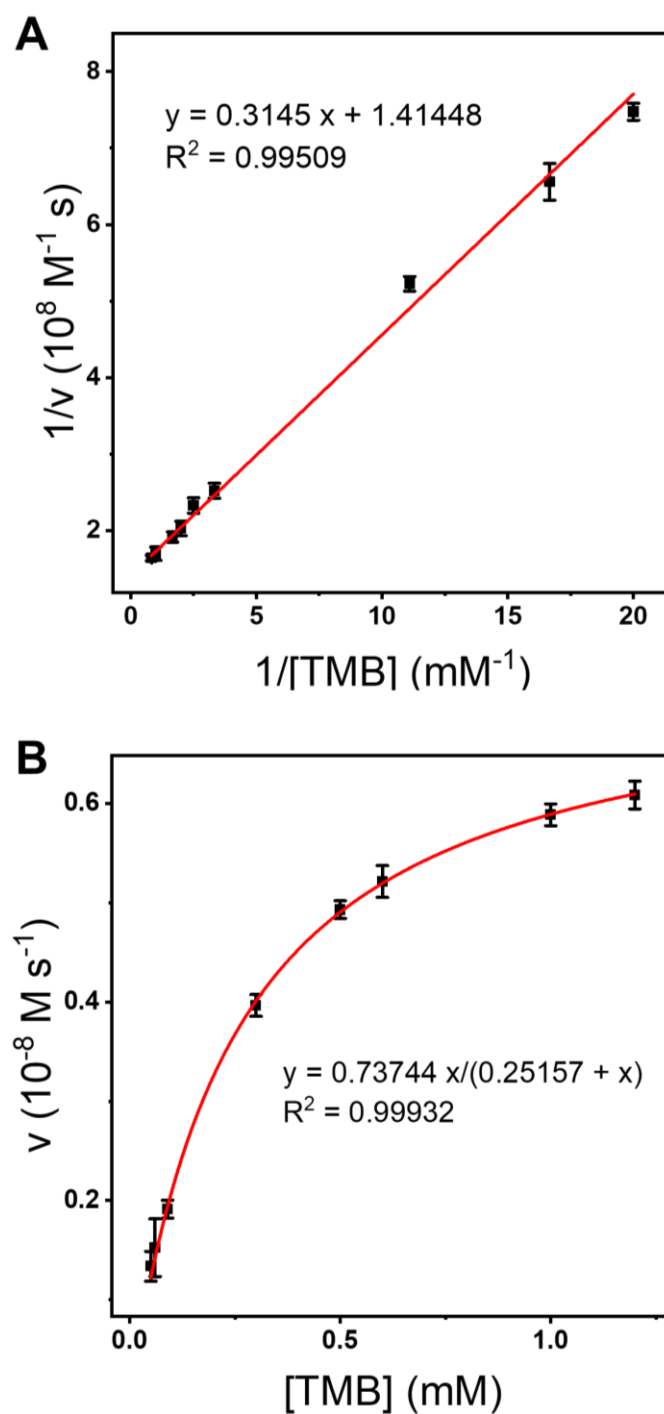


Fig. S7. (A) Double reciprocal plot and (B) Michaelis-Menten curve for enzyme inhibition kinetics of Fe-MOF with 0.5 μ M of methidathion.

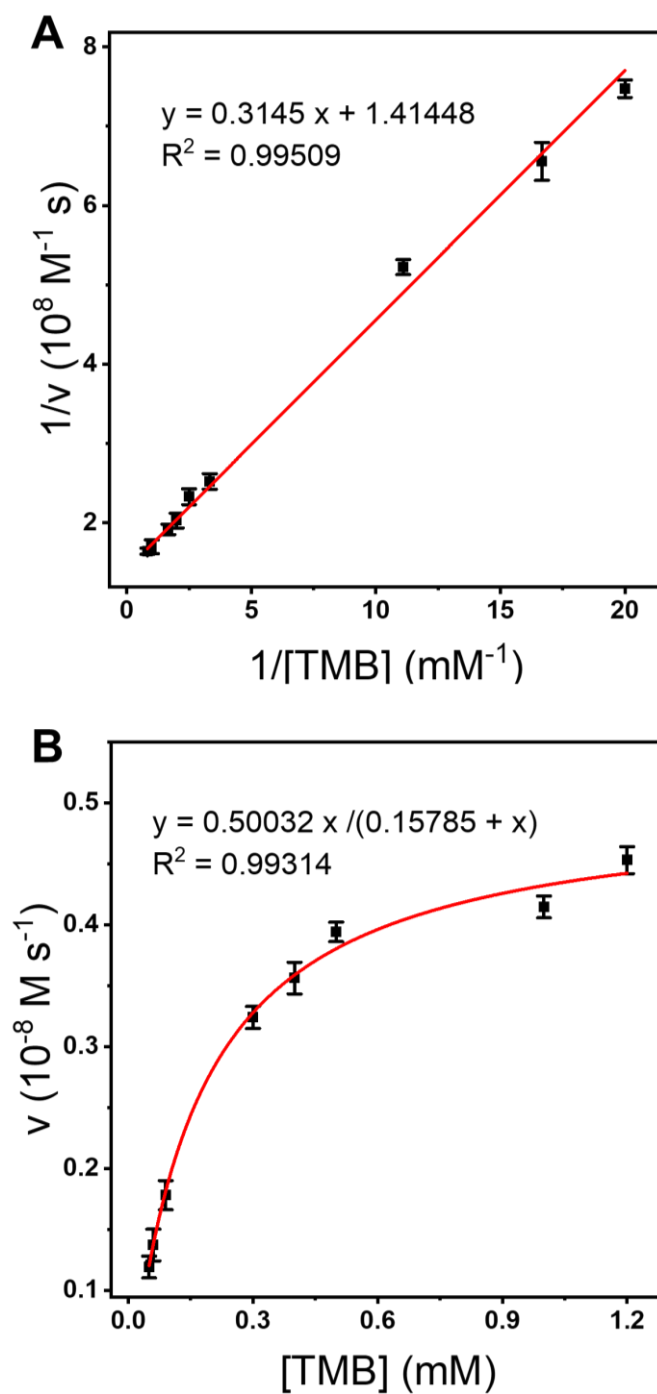


Fig. S8. (A) Double reciprocal plot and (B) Michaelis-Menten curve for enzyme inhibition kinetics of Fe-MOF with 1 μM of methidathion.

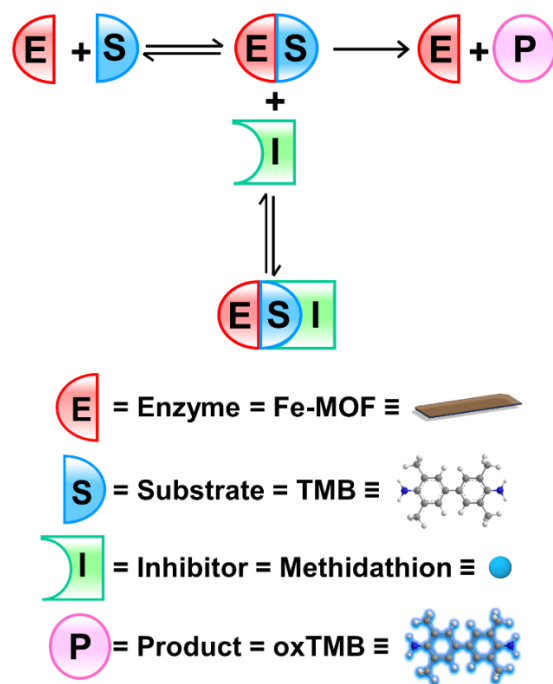


Fig. S9. Schematic of the steady-state equilibrium for uncompetitive inhibition.

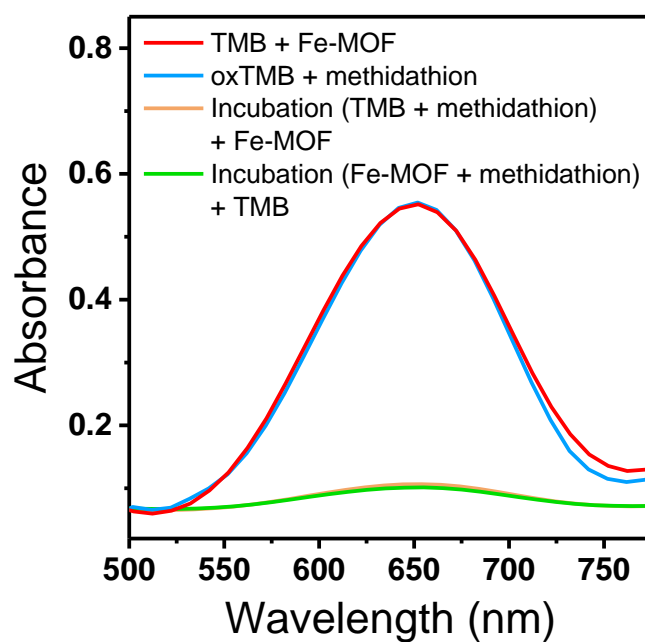


Fig. S10. Absorbance spectra of various reaction systems for oxidase-like activity of Fe-MOF. The incubation of TMB+methidathion and Fe-MOF+ methidathion were conducted for 10 min, followed by an activity assay.

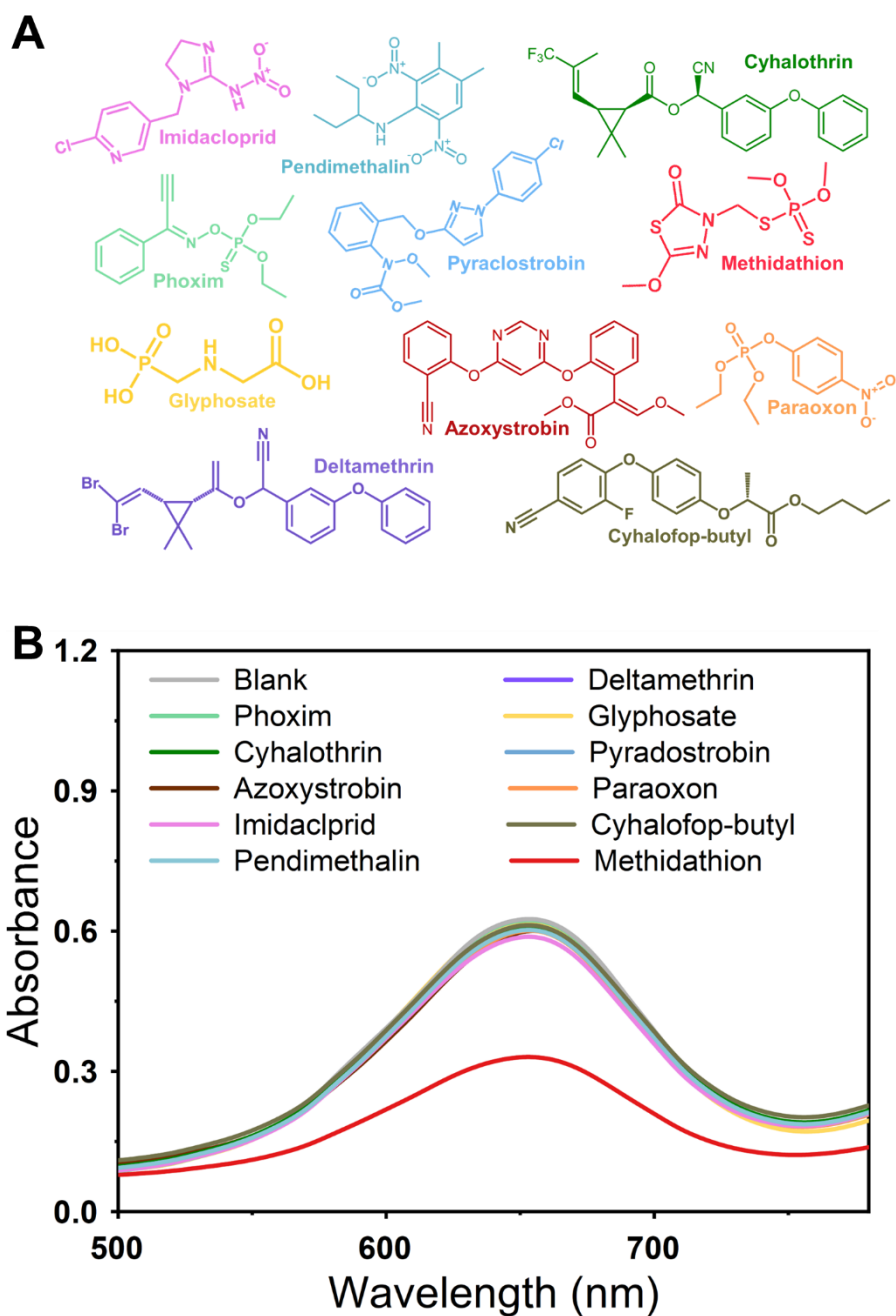


Fig. S11. The activities of Fe-MOF after incubation with the various pesticides. (A) Structural formulas of used pesticides. (B) Absorption spectra of the catalytic reaction of Fe-MOF after incubation with various pesticides.



Fig. S12. Photograph of the reaction system with various concentrations of methidathion.

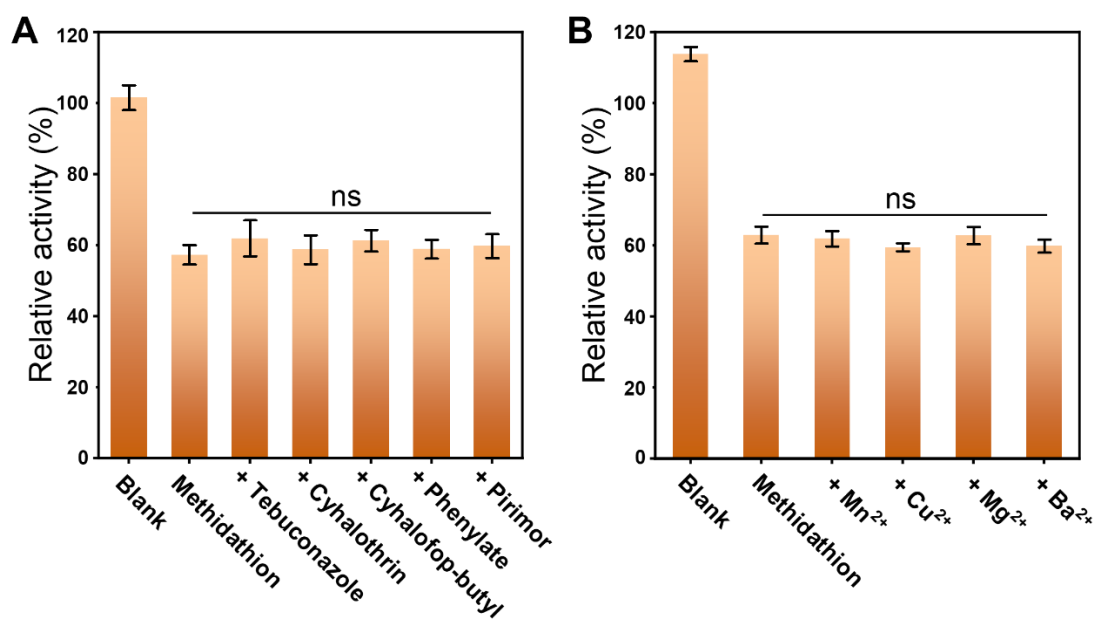


Fig. S13. Signal response of the colorimetry system for methidathion detection in the presence of (A) other pesticides (0.1 mM) and (B) metal ions (0.1 mg/mL).

Table S1. Performance comparison of various analytical methods

Method	Material ^a	Concentrations of materials (mg/mL) ^b	Target	LOD (nM)	Linear range (μM)	Ref.
Electrochemistry	MIP/sol-gel	/	Methidathion	20	0.13–0.66	1
Electrochemistry	Ag@rGO-NH ₂	1	Methidathion	31.42	0.04–0.35	2
Electrochemistry	NCGCE	/	Methidathion	30	0.05–0.7	3
Electrochemistry	Ag/GNPs/ZrO ₂	/	Nitroaromatic organophosphorus pesticides	100	1–20	4
Electrochemistry	NiCo ₂ O ₄ -PAMAM-peptide	/	Methyl paraoxon	80	0.2–100	5
			Ethyl paraoxon	160	0.5–100	
Fluorescent	TPE-Peptide	/	Organophosphorus pesticides	600	1–100	6
Colorimetry	Au NPs	/	Dimethoate	17	0–0.15	7
Colorimetry	Fe-MOFs	0.1	Methidathion	5.48	0.01–1.4	This work

^a MIP, molecularly imprinted polymers; rGO-NH₂, amine functionalized reduced graphene oxide; NCGCE, Nafion®-coated glassy carbon electrode; GNP, graphene nanoplatelet; PAMAM, polyamidoamine; TPE, tetraphenylethylene; NPs, nanoparticles; Fe-MOFs, Iron-based metal-organic frameworks.

^b ‘/’ indicates that it was not mentioned in the corresponding reference.

Table S2. Determination of methidathion in real samples

Sample	Content (μM)	Spiked (μM)	Found (μM)	Recovery (%)	RSD ^a (%, n=5)
Tap water	0	0.1	0.104 ± 0.002	104	1.9
		5	5.05 ± 0.1	101	2.0
		14	14.03 ± 0.23	100.2	1.6
River water	0	0.1	0.103 ± 0.004	103	3.9
		5	4.97 ± 0.09	99.4	1.8
		14	14.06 ± 0.22	100.4	1.6
Sea water	0	0.1	0.097 ± 0.004	97	4.1
		5	4.95 ± 0.11	99	2.2
		14	13.93 ± 0.2	99.5	1.4

^a For each sample, the experiment was repeated five times and “ \pm ” represents the standard deviation (n = 5).

References

- (1) Bakas, I.; Hayat, A.; Piletsky, S.; Piletska, E.; Chehimi, M. M.; Noguer, T.; Rouillon, R. *Talanta* **2014**, *130*, 294-298.
- (2) Guler, M.; Turkoglu, V.; Basi, Z. *Electrochim. Acta* **2017**, *240*, 129-135.
- (3) Erdoğan, G. *J. Anal. Chem.* **2006**, *61* (7), 673-676.
- (4) Ulloa, A. M.; Glassmaker, N.; Oduncu, M. R.; Xu, P.; Wei, A.; Cakmak, M.; Stanciu, L. *ACS Appl. Mater. Inter.* **2021**, *13* (30), 35961-35971.
- (5) Yang, Y.; Hao, S.; Lei, X.; Chen, J.; Fang, G.; Liu, J.; Wang, S.; He, X. *J. Hazard. Mater.* **2022**, *428*, 128262.
- (6) Wang, J.; Zhang, J.; Wang, J.; Fang, G.; Liu, J.; Wang, S. *J. Hazard. Mater.* **2020**, *389*, 122074.
- (7) Liu, S.; Zhao, J.; Wu, J.; Wang, L.; Hu, J.; Li, S.; Zhang, H. *Anal. Bioanal. Chem.* **2023**, *415* (29), 7127-7138.